# Supplemental Information to

# Ultrasensitive electrochemiluminescence detection of DNA based on nanoporous gold electrode and PdCu@carbon nanocrystals composites as labels

Mei Yan [a], Meng Zhang [a], Shenguang Ge [b], Jinghua Yu [a,*], Meng Li [a], Jiadong Huang [a], Su Liu [a]

([a] Key Laboratory of Chemical Sensing & Analysis in Universities of Shandong(University of Jinan), Chemistry and Chemical Engineering, University of Jinan, Jinan 250022, China;

[b] Shandong Provincial Key Laboratory of Fluorine Chemistry and Chemical Materials, School of Chemistry and Chemical Engineering, University of Jinan, Jinan 250022, China)

[*]Corresponding to: Jinghua Yu

E-mail: ujn.yujh@gmail.com

Fax: +86-531-82765969

# 1 X-ray diffraction(XRD) of PdCu alloy

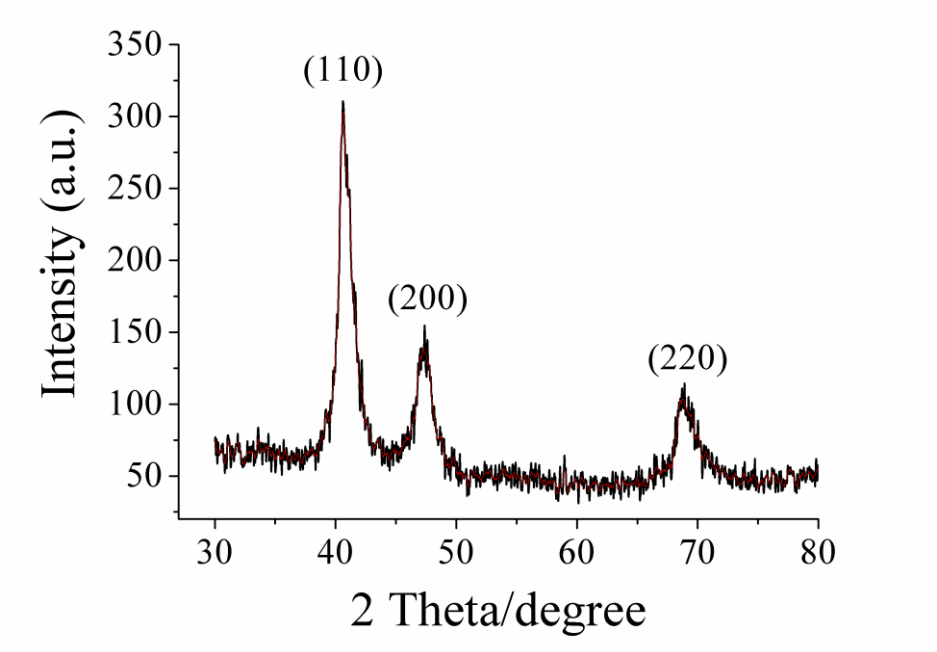


Figure S. 1 XRD pattern for PdCu alloy

As shown in Figure S.1, the peaks can be assigned to the diffraction of the (111), (200), and (220) planes of face-centered cubic. The well-defined diffraction peaks sit well within the range of the diffractions for PdCu bimetallic nanostructure, indicating the formation of a PdCu alloy structure.

# 2 Characterization of CNCs

## 2.1 Absorption and PL spectra of CNCs

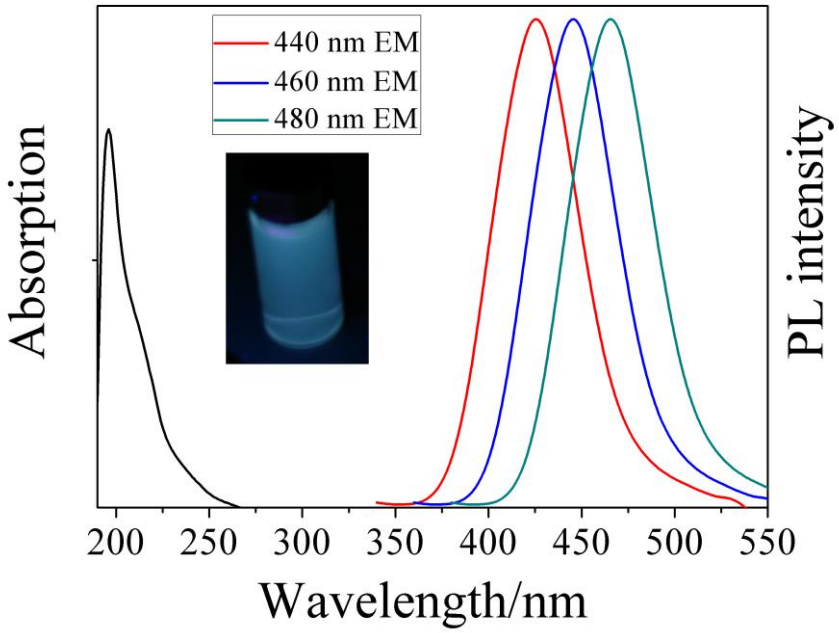


Figure S. 2 UV-vis sbsorption and PL spectrum (recorded for progressively longer emission wavelengths from 440 to 480 nm in 20 nm increments) of CNCs in acqueous solution. PL spectrum was obtained under excitation at 365 nm. Inset is the solution illuminated by a UV lamp.

The UV-vis absorption spectrum revealed that the first absorption band occurred at 200 nm. The PL spectra ranged from 440 (blue) to 560 nm (yellow) with increase in the diameter.corresponding to the photoluminescent quantum yield of 27.0 %, 18.1 % and 12.3 %, respectively. The inset showed the bright blue emission (EM) from the product excited by a UV lamp as we monitored the electrolyte solution during the electrochemical process (Figure S. 2).

## 2.2 The photoluminescence quantum yield (QY)

Rhodamine 6G was used as the reference material. The QY is defined as

$$Y_u = Y_s \cdot \frac{F_u}{F_s} \cdot \frac{A_s}{A_u}$$

Where $Y_u$ and $Y_s$ are the QY of CNCs and rhodamine 6G, $F_u$ and $F_s$ are the integral area of fluorescence of CNCs and rhodamine 6G, $A_u$ and $A_s$ are the absorption of CNCs and rhodamine 6G, respectively.

The QY of CNCs from 440 (blue) to 560 nm (yellow) was 27.0 %, 18.1 % and 12.3 %, respectively. The as-prepared CNCs with blue EM was chosen in this assay.

## 3 Characterization of the NPG-based DNA biosensor

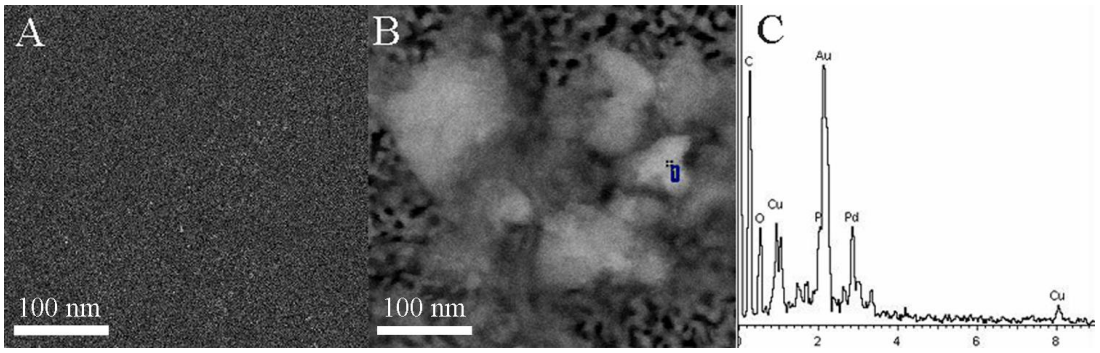


Figure S. 3 Characterization of the NPG-based DNA biosensor. (A) SEM image of GCE; (B) SEM image of NPG modified GCE hybridization with the PdCu@ CNCs labeled reporter DNA; (C) EDS of NPG modified GCE hybridization with the PdCu@ CNCs labeled reporter DNA.

The morphology of glassy carbon electrode (GCE) and hybridization with the PdCu@ CNCs labeled reporter DNA was characterized Figure S.3. As can be seen from the SEM images (Figure S. 3, A), the bare GCE was smooth. When NPG was assembled on the surface of GCE, the PdCu@ CNCs labeled reporter DNA was also hybridized with target DNA, thus assembled on the surface of GCE (Figure S. 3, B). The composition analysis with energy dispersive spectrometer (EDS) gave a nominal composition of NPG modified GCE hybridization with the PdCu@ CNCs labeled reporter DNA (Figure S. 3, C).

## 4 Incubation time of PdCu@CNCs composites and $S_3$

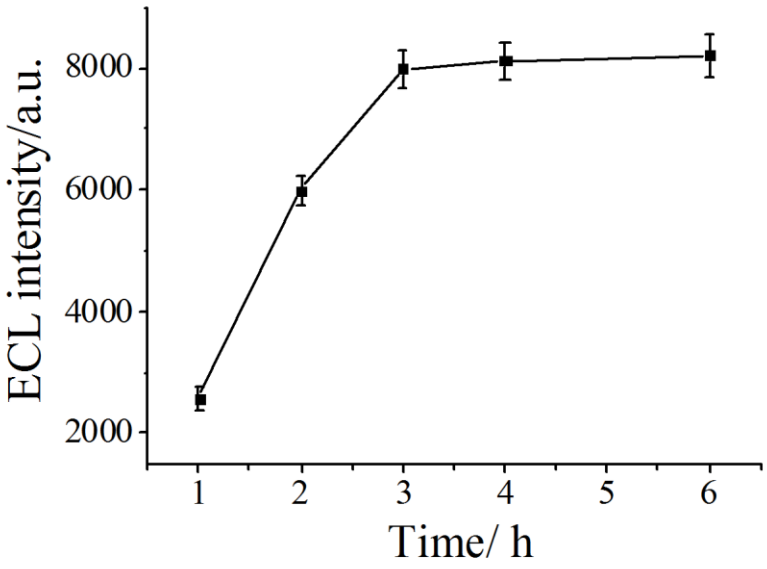


Figure S. 4 Effect of incubation time of PdCu@CNCs composites and $S_3$

The effect of incubation time on the DNA biosensor was performed. As shown in Figure S. 4, the effect of incubation time of PdCu@CNCs composites and $S_3$ was studied in the range of 1, 2, 3, 4, and 6 h. The results showed that the ECL intensity of the DNA biosensor reached a maximum value when the time comes to 3 h, then the current signal begins to level off. It suggests that the optimal incubation time of PdCu@CNCs composites and $S_3$ is 3 h.

## 5 Hybridization temperature of $S_1$ and $S_2$

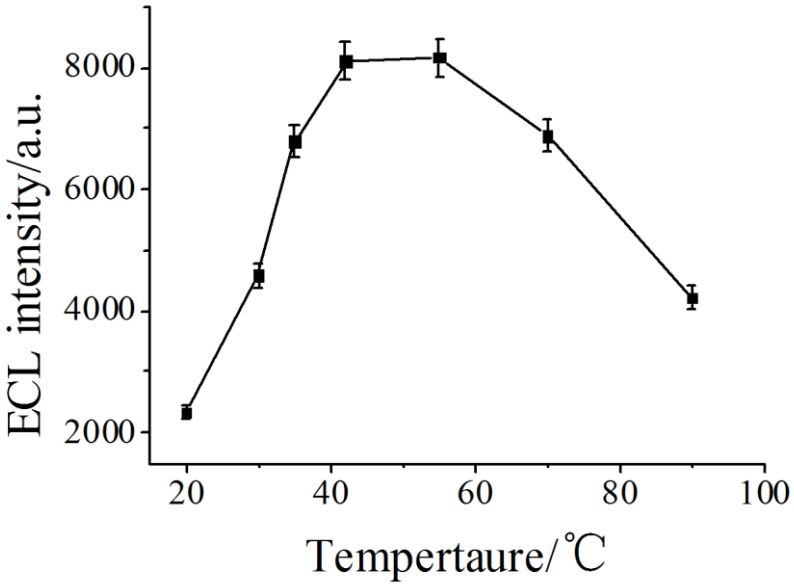


Figure S. 5 Effect of of hybridization temperature of $S_1$ and $S_2$

The effect of hybridization temperature of $S_1$ and $S_2$ on the hybridization reaction was performed (Figure S. 5). As shown in Figure S. 3, the effect of hybridization temperature of $S_1$ and $S_2$ was studied in the range from 20-90 ℃. The results showed that the ECL intensity of the DNA biosensor reached a maximum value at 42 ℃, indicating that the optimal incubation temperature of $S_1$ and $S_2$ occurred at 42 ℃.

## 6 Hybridization temperature of $S_2$ and $S_3$

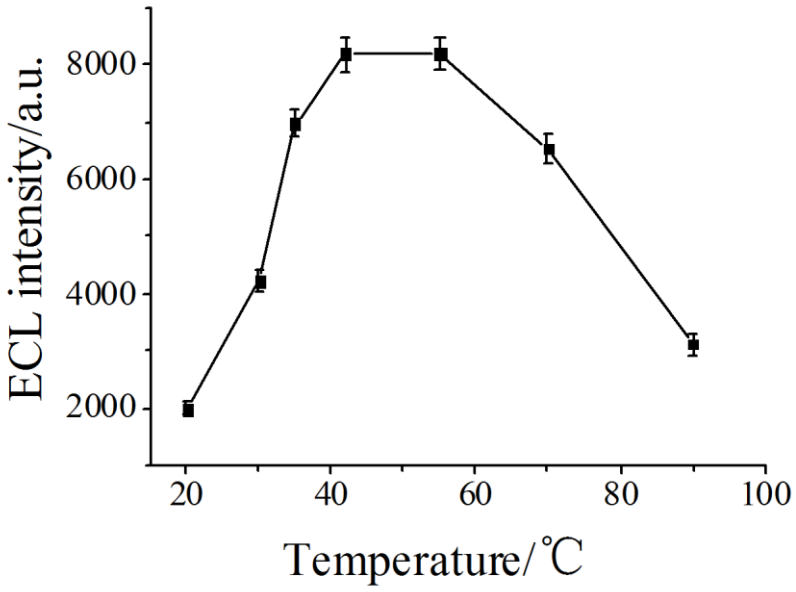


Figure S. 6 Effect of of hybridization temperature of $S_2$ and $S_3$

The effect of hybridization temperature of $S_2$ and $S_3$ on the hybridization reaction was performed (Figure S. 6). As shown in Figure S. 4, the effect of hybridization temperature of $S_2$ and $S_3$ was studied in the range from 20-90 ℃. The results showed that the ECL intensity of the DNA biosensor reached a maximum value at 42 ℃, indicating that the optimal incubation temperature of $S_2$ and $S_3$ occurred at 42 ℃.

## 7 Regeneration of the DNA biosensor

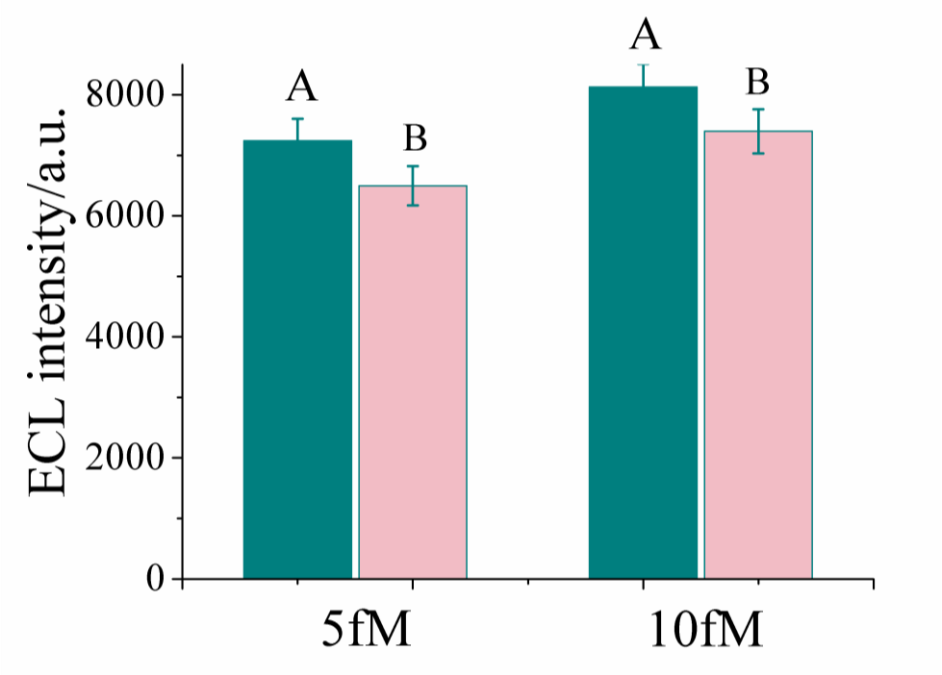


Figure S. 7 Comparison of ECL signals for unheated electrode (A) and heated (90 ℃ for 1 min) electrode (B) hybridized with a series of target DNA for 5 fM and 10 fM, respectively. Error bars showed the standard deviations of measurements.

In our test, the DNA biosensor could be regenerated by incubation of the modified electrode in hot water (90 ℃) for 1 min, by which hybridized DNA was removed via thermal denaturation. As shown in Figure S. 7, the as-renewed electrode could restore 89.7 %, and 91 % of the initial value for unheated modified electrode at $S_2$ concentrations of 5 fM and 10 fM, respectively. The electrode was evaluated by five replicative measurements, showing accepted reusability. The consecutive measurements were repeated five times and a RSD of 5.2 % was acquired, indicating a good repeatability. The DNA biosensor could be stored in the refrigerator for one week with negligible loss of the immobilized probe DNA.